15

An Active Technology for Improving the Sound Transmission Loss of Glazed Facades

Berardo Naticchia, Alessandro Carbonari and Sara Spadoni
Polytechnic University of Marche
Department of Architecture Construction and Structures
Italy

1. Introduction

The 89/106/CEE European Directive and the related national legislation of the European member countries have made noise protection a compulsory building requirement. From an acoustic point of view, building envelopes have the task of reducing external noise to an acceptable level inside the same building.
In fact, glazed facades are the preferred paths followed by disturbing noise from the outside to the inside and, in spite of the adoption of very expensive passive means, they are often unable to respect the strict limits required by standards and regulations. The two main types of passive means used are: laminated glass technology or double glazing. Both of these can be useful for reducing noise transmission at high frequencies: in particular the laminated solution is used to shift the coincidence effect at frequencies higher than the audible range, in fact improving STL values in the range of acoustic waves higher than 1500 Hz, while determining no improvements at lower frequencies. On the other hand, in double glazing, the coupling between the glass panels and the air layer adds another resonance effect at frequencies lower than 500 Hz, while improving their STL in the range of frequencies limited between the resonance and coincidence effects. As a consequence, the adoption of an active control system is needed to solve the acoustic performances drop of glass panels at low frequencies.
This chapter will show how an active system would be capable of controlling the vibrations of glazed panels and of reducing sound radiated as a consequence, avoiding the use of very expensive glazed facades equipped with massive passive means and effective only at high frequencies, whose adoption would also raise economic and technologic problems for their installation on buildings. In particular, the ASAC (Active Structural Acoustic Control) approach will be analyzed and tested, also demonstrating why it is better than the other Active Noise Control approach, commonly known as ANC. Pursuing this aim requires tackling a series of complex problems such as choosing reference and error sensors, modelling the system controller, designing the system with well-suited actuators, integrating the active system into typical glazed façades while minimizing visual impact and maximizing the controllability of structural vibrations. It will be shown that remarkable sound transmission loss (STL) improvements can be obtained and that this approach has great exploitability potential in other specialized products like light opaque building partition walls, railway and traffic noise shielding, temporary environmental noise barriers or even real-time controlled reflecting panels for the acoustic adjustment of concert halls.

2. State of the art and the innovation provided by ASAC systems for glass panels

2.1 Early Active Noise Control applications

The concept of active noise control was first introduced by Leug (Leug, 1936), who presented a patent for a system implementing feed-forward active control of sound in a duct. According to the patent, the sound field is detected using a microphone, whose signal is passed through an electronic controller, such that it adjusts the loudspeaker to produce a cancelling wave in a duct, resulting in destructive interference of the primary or noise source wave. A feed-back arrangement was produced by Olson and May (Olson et al., 1953), who developed an active noise control system that is based upon detecting the offending sound with a microphone and feeding the signal back through a controller to a control loudspeaker located close to the microphone. They also demonstrated good local reduction at the microphone over a range of frequencies from 20 to 300 Hz.

Conover (Conover, 1955) introduced the concept of an error sensor in which the radiated sound field of the transformer was monitored and used to adjust the controller in order to minimize the radiated sound. However, he experienced difficulties due to the use of analogue systems, particularly when the physical system was changing relatively rapidly.

Hence, in the early 1970s both (Kido, 1975) and (Chaplin et al., 1976) began exploring the application of digital signal processing techniques, demonstrating the feasible use of their digital active noise control approaches on a number of important applications, such as car exhaust noise, ship exhaust stack noise and active engine mounts.

2.2 Active control of structural vibrations

The introduction of digital techniques and piezoelectric actuators to vibration control by Bailey & Hubbard (1985) considered feedback modal control of large structures. Balas & Canavin (1977) discussed feedback damping control of large spacecraft structures. Balas (1978) applied theoretical modal control using velocity feedback to a simple beam. Meirovitch & Öz (1980), with later work by Meirovitch and others (e.g. Meirovitch et al., 1983), expanded the modal control method, finally arriving at a method they described as Independent Modal-Space Control (IMSC), where a coordinate transformation was used to decouple a complicated system into a set of independent second order systems in terms of modal coordinates.

Baz & Poh (1988) made modifications to the IMSC method to minimize the effect of control spillover (inadvertent localized increases in vibration levels due to constructive interference between disturbance and control fields). Modern applications include precision optical components in noisy environments, pilot seat vibrations in helicopters, sonar masking in torpedoes and submarines.

2.3 Active Structural Acoustic Control

Advances in active control of structural vibrations have been applied to develop an alternative control method for enclosed noise fields, known as active structural acoustic control (ASAC). The ASAC approach uses structurally-based actuators to exert control forces on the radiating structure itself in order to minimize radiated sound (Ruckman & Fuller, 1995; Nelson & Elliott, 1995; Fuller et al., 1996). The actuators are vibration sources (shakers, piezoceramic patches, etc.) which modify how a structure vibrates, thereby altering the way it radiates noise.

In 1990 Jones and Fuller proposed an initial work where electromagnetic shakers were used to provide point force control inputs to simplified cylindrical test sections. The controller exploited error sensor microphones placed in the cylinder interior, such that interior sound levels were minimized by the control of structural vibration. This work demonstrated that, in general, fewer control actuators are required by the ASAC approach as compared to ANC (Active Noise Control) techniques. Also, control spillover in the interior acoustic space was reduced in the ASAC experiments. In such cases, "modal suppression" is usually suggested, where only the few dominant radiating modes are reduced in amplitude. Other structural modes that are poorly coupled with the noise field may be left unchanged by the control system (Fuller et al., 1996).
Simpson, et al. (1991) performed control experiments in a test section comprising the aft portion of a furnished DC-9 aircraft. Using a typical feed-forward controller arrangement, the researchers achieved global sound level reductions of up to 9 dB using various configurations of 7 error microphones.
Because point forces are spectrally white in a spatial sense, their use as controlling forces in ASAC work can lead to undesired spillover in many structural vibration modes. In seeking a control actuator with more distributed forcing properties, many researchers recently investigated the use of piezoceramic materials for applying bending moments or in-plane strains to structures (Clark et al., 1991). In particular, lead zirconium titanate (PZT) materials have been widely used in ASAC work, providing sufficient forcing capabilities with the benefit of greatly reduced mass and space requirements as compared to electromagnetic shaker devices.
In 1992 Fuller et al. used an aluminium cylindrical test section with a removable floor structure to simulate an aircraft fuselage environment. Piezoelectric patches were bonded directly to the cylinder surface and the system was acoustically excited with an exterior loudspeaker noise source. Using two microphones as error sensors, the ASAC system provided global attenuations on the order of 10 dB in the cylinder interior.
Recently, ASAC tests were performed by Fuller et al. (1994) in the cabin of a Cessna fuselage, a typical mid-sized business jet. In the acoustic resonance case, noise reductions of 20 dB or more were achieved at the error sensors, but an average global increase of several dB was measured at 7 additional microphones. Control performance in the off-resonance case was significantly reduced, with reductions of 2-10 dB at the error sensors.
Some past work has addressed actuator position optimization via analytical approaches (Clark et al., 1992; Wang et al., 1994; Burdisso et al., 1994). Additionally, one work with a finite element model has shown the importance of position optimization to global ASAC performance, made by (Yang et al., 1995). Spatially averaged reductions of acoustic potential energy of up to 14 dB have been predicted using 16 optimally-located point forces, while poor control force placement may result in overall global sound increases.

2.4 Active Noise Control in glazed enclosures

To the authors' knowledge, no ASAC application has been performed on glazed structures. Other works by (Kaiser et al., 2003) suggest an ANC approach through the positioning of both loudspeakers and sensors inside air cavities; and (Zhu et al., 2004) place monitoring sensors outside windows. Instead, most of the recent research was developed to verify the performances of the control provided by PZT patch actuators on opaque surfaces, both for building walls and for helicopter and airplane envelopes: in the contributions of (Kaiser et

al., 2003) and (Bao and Pan, 1997) it is shown that using ANC control systems for double walls needs cavities wider than 0.1 m thick, which is not usual for standard double glazed panels. Preliminary results in Wernli (2001) show that PZT laminated (multi-layer) patches can indeed actuate the heavy panes sufficiently. However, since these patches interfere substantially with the primal function of the window, namely to look through it, they may not be considered an option.

2.5 The original contribution provided by the proposed ASAC system for glass panels

The research described in this chapter proposes an original approach for applying ASAC on glazed structures, which takes into account the problem of using piezo stack actuators, whose visual impact must be managed, even if considerably reduced compared to the piezo-laminated patch actuators.

The application of ASAC systems on glazed panels is particularly critical, as there are no means of efficiently increasing their STL over all the acoustic spectrum, as will be explained in paragraph 3.1. For example, acoustic interlayers provide the most significant noise reduction in the frequency range of 1500 to 6000 Hz, while in the range of 100 to 500 Hz the Sound Transmission Loss remains significantly low. Furthermore, the double glazing approach provides appreciable noise reduction just in the frequency range above 500 Hz.

Hence the use of the ASAC technology seems to be the only one capable of increasing glazed facades' STL over all the acoustic spectrum. In this way, it would be possible to respect the strict European and national legislation on expected acoustic performance for external facades, even in very harsh areas, such as in proximity of airports, railways or high traffic roads. Additionally, the problems connected with the application of actuators on transparent facades will be tackled for the first time.

3. Adoption of active means for controlling acoustic and vibration behaviour of glass panels

3.1 Adoption of active means for STL increase

Considering that for buildings, the main type of disturbing noise is produced by road and railway traffic, panels excited by plane waves have been studied. Analytical solutions for forecasting the behaviour of unbounded non flexible panels are known (Fahy, 1985), and they can be easily extended to building envelopes. The STL of glass alone at low frequencies is determined by the panel's static stiffness. Since glass reacts best to excitation frequencies that match its natural frequencies, the low internal damping of tempered glass produces resonances that dramatically decrease its STL. Above the resonant frequencies, sound transmission follows the mass law of acoustics and is dictated by the mass or surface density of glass. However, glass has a specific coincidence frequency at which the speed of incident acoustical waves matches that of the glass bending wave and acoustic waves are especially effective at causing glass to vibrate, which makes the vibrating glass an effective sound radiator at that specific frequency and above. As a result, the first critical point for a single glass panel is in correspondence of the resonance effect (f_R), registered at very low acoustic frequencies, as in Fig. 1-a (Spagnolo, 2001). Above this value its STL increases with frequency, until the critical effect causes another drop of STL, due to the matching between the wavelength of flexural vibrations propagating through the glass and the projection of the disturbing noise wavelength which dramatically increases the overall radiation efficiency of the glass panel. The latter effect may be solved through the adoption of

laminated glass panels with PVB layers, which decrease the overall flexural stiffness of laminated panels, shifting up the critical frequency (f_C), out of the audible range. But no remarkable improvements are obtained at the resonance frequency. Even if double glazing provides an average increment of STL (moreover in the middle frequency range), however it generates another resonance frequency, due to the coupling between the two glass panels and the air cavity, whose position depends on the thickness and typology of the panels (Harris, 1984). An illustrative example from measurements is presented in Fig. 1-b, based on (Harris, 1994): three double glass panels are compared in order to point out the importance of the air layer thickness with respect to the final STL. Starting from a good double glazing (two 0.006 m thick glass panels with a 0.013 m air layer interposed) it is demonstrated that even if the air layer is further widened, the low frequency STL is still low due to resonance dip which persists even if a much higher air thickness equal to 0.05 m is provided.

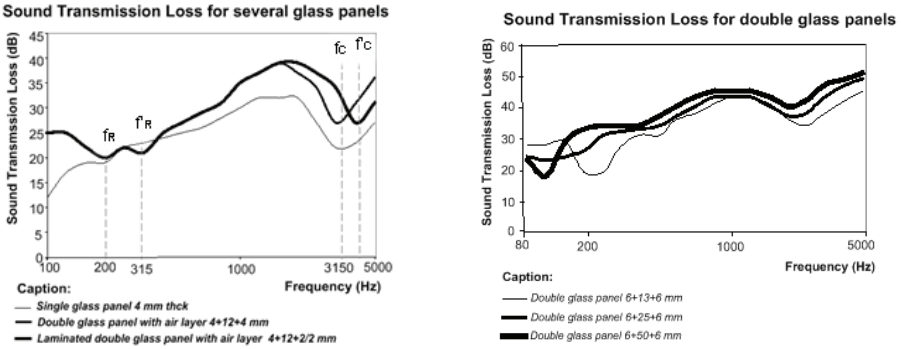

a) b)

Fig. 1. Sound Transmission Loss curves for single, double and laminated glass panels (a); the same for double glass panels (b).

Moreover, considering that traffic noise levels are usually very high in the low frequency range (IMAGINE, 2003), it follows that other solutions are required for guaranteeing acoustic comfort in buildings (as illustrated in Fig. 2).

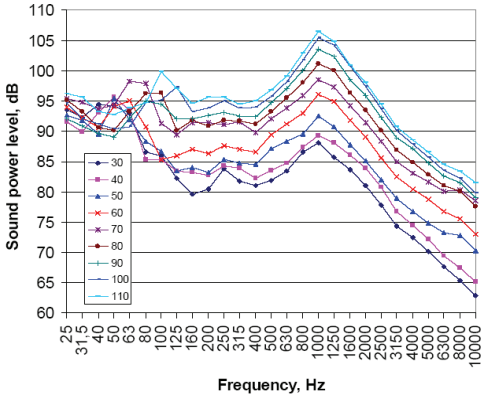

Fig. 2. Equivalent omni-directional sound power level of road traffic noise as function of a vehicle's speed.

3.2 Analytic model for the simulation of vibrating glass panels

As flexural waves in structures are the main responsible agents for sound emission (Hall, 1987) and they are induced in plates by external disturbances, it is opportune to analytically describe the flexural response of a simply supported plate to a harmonic excitation of arbitrary distribution like $f(x,y,t) = F(x,y)\,e^{i\omega t}$ (where $\omega = 2\pi\nu$, ν is the excitation frequency, $F(x,y)$ is the excitation amplitude), obtaining the equilibrium model introduced by Kirchhoff-Love (Timoshenko and Woinolowsky-Krieger, 1959):

$$EI\left(\frac{\partial^4 w}{\partial x^4} + 2\frac{\partial^4 w}{\partial x^2 \partial y^2} + \frac{\partial^4 w}{\partial y^4}\right) + \rho h \frac{\partial^2 w}{\partial t^2} = -F(x,y)e^{i\omega t} \tag{1}$$

being i the complex unit, w the transversal displacement, E, I, ρ and h the elasticity modulus, moment of inertia, density and thickness, respectively, of the plate. One of the possible solutions of eq. (1) for the formalization of the transverse displacement field is obtained describing it as the superposition of infinite modes of the free response of the plate, which is vibrating at the forcing frequency:

$$w(x,y) = \sum_{m=0}^{\infty}\sum_{n=0}^{\infty} W_{m,n}\Psi_{m,n}(x,y)e^{i\omega t} \tag{2}$$

where $W_{m,n}$ are the modal amplitudes, which are the maximum displacements at the free natural mode *(m, n)*. $\Psi_{m,n}$ are the modal shapes, which take into account the shape of the mode *(m,n)* on the plate, while the exponential term is aimed at describing the dependence with the time and the influence of disturbing frequency. In order to study the transversal displacement motion of a plate whose side lengths are a and b, it is necessary to compute the displacement distribution field given by an incident plane wave. Eq. (2) is generally approximated in another form, which considers only the superposition of a finite number of vibrating modes, given by the combination of two finite numbers m and n (the validity of the approximation is dependent on the choice of these two values). Thus the displacement distribution is given by (Fuller et al., 1997):

$$w(x,y,t) = \sum_{m=1}^{M}\sum_{n=1}^{N} W_{m,n}\,\mathrm{sen}(k_m x)\cdot \mathrm{sen}(k_n y)e^{i\omega t} \tag{3}$$

where the eigenvalues are:

$$k_m = \frac{m\pi}{a},\ k_n = \frac{n\pi}{b} \tag{4}$$

Substituting eq. (3) in eq. (1) we can find the solution as:

$$W_{m,n} = \frac{P_{m,n}}{\rho h\left(\omega_{m,n}^2 - \omega^2\right)} \tag{5}$$

being $P_{m,n}$ the modal pressure, that is, the action given separately by each mode of vibration, $\omega_{m,n}$ the natural frequencies of the glass plate as reported in (Fahy, 1985):

$$\omega_{mn} = \sqrt{\frac{EI}{\rho h}\left[\left(\frac{m\pi}{a}\right)^2 + \left(\frac{n\pi}{b}\right)^2\right]} \tag{6}$$

In (Roussos, 1985) an analytical solution for the generic case of a plane wave incident on a simply supported plate, like in Fig. 3, is detailed.

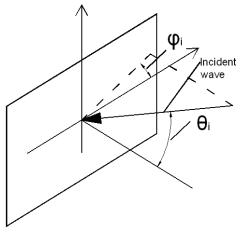

Fig. 3. Angles individuating the direction of incidence of an acoustic plane wave into a glazed plate.

4. The ASAC active control system adopted

4.1 Active Structural Acoustic Control

The approaches by Leug's patent in 1936 and (Olson & May, 1953) are the first examples of ANC feed-forward control, when prior knowledge of the noise is obtained with an upstream microphone, and ANC feedback arrangement, where the detection microphone is close to the active secondary source respectively. Both approaches relate to the main concept of ANC, and hold its drawbacks: when applied to buildings' glazed facades, they need an external microphone for disturbance monitoring, and internal error sensors and loudspeakers for control purposes. For this reason some attempts at inserting all the system components inside the air cavity of double walls were pursued but this task became much too difficult in the case of windows, due to their narrow air layers.

Therefore, the ASAC system should be preferred for this kind of application, because both reference sensors and actuators are placed on the same glazed panel, as required for the implementation of a feedback controller. Fig. 4-a and Fig. 4-b respectively depict the feed-forward and feed-back arrangements of an ASAC configuration for glazed facades' control. In both cases, actuators are positioned on the vibrating surface, which is the source of disturbing noise in the receiving room and whose vibrations are reduced to rise its final STL. ASAC does not require the use of loudspeakers or error microphones in the receiving environment, however optimum positioning of sensors and PZT actuators on the vibrating surface must be pursued. Generally, various modes of vibration have different radiation efficiencies (Fahy, 1985), and some are better coupled to the radiation field than others. This suggests two conclusions: only the most efficient modes need to be controlled, rather than the whole response; in some cases the relative phases and amplitudes of multi-modal response can be adjusted so that their radiated fields interfere destructively.

The feed-forward control of Fig. 4-a requires knowledge of the primary disturbance, which is derived by the use of a reference microphone: in the case of buildings, this seems unpractical, because it would require the installation of a microphone on the exterior of the

window which, for functional and aesthetic issues, is not feasible. Therefore, the feedback type controller depicted in Fig. 4-b seems to be opportune and is detailed subsequently.

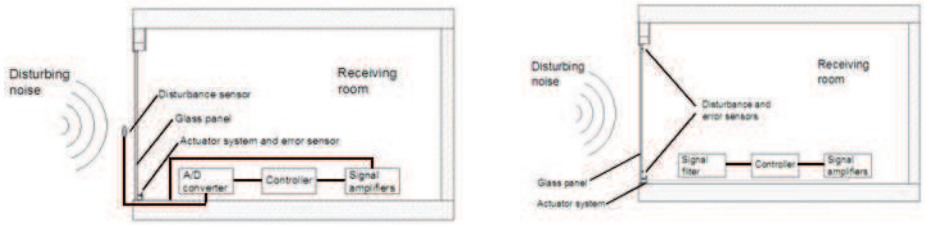

a) b)

Fig. 4. Feed-forward (case a) and feedback (case b) ASAC systems for glazed facades.

4.2 Optimal control theory

The ASAC approach is based on the reduction of structural vibrations and radiated sound (transmitted and reflected) as a consequence, by means of actuators bonded on the vibrating surfaces. ASAC can be easily integrated into buildings, as it does not require the use of loudspeakers or error microphones in the receiving environment.

As shown in Fig. 5, once the signal comes from the sensors, it must be elaborated by charge amplifiers (converting voltage signals into physical variables like displacements, velocity and accelerations), and electronic filters that have a double task:

- to separate the contribution to the total vibration field due to the primary disturbance from that due to secondary sources;
- to compute the radiated field in some positions of the receiving room, to calculate the error (difference between reference value and actual value of the radiated noise).

The controller, starting from the error signals, computes the opportune voltage to be supplied to the secondary sources, whose electric power is provided by the amplifiers. At this level an algorithm calculates the control voltage to be supplied to the secondary sources. In general, it has the task of changing the distributed mass, stiffness and damping of the plate in order to reduce the radiated noise in the internal environment, determined mainly by flexural waves which need to be decreased by the control plant for this reason. The complexity of the algorithm derives from the fact that reference and control sensors are positioned at the same place, therefore electronic filters are necessary. The controller must opportunely tune its gain coefficients to adjust the properties of the system, so that the radiated noise will be minimized. A number of papers, such as (Baumann et al., 1992), (Cunnefare, 1991), (Baumann et al., 1991) and (Pan et al., 1992), showed that optimum control is the most suitable for ASAC systems: it has the advantage that the choice in the prescribed change of the dynamic properties is motivated by its aim to reduce structural vibrations or radiated noise.

Optimal control system procedures offer the possibility of designing the controller parameters directly minimizing a cost function of performance which is proportional to the required measure of the system's response. For the sake of computational efficiency, it is convenient to define a cost function that is quadratically dependent on the response, simplifying the optimization problem. One of the possible solutions can be the one proposed by (Fuller et al., 1997), where the cost function is given by:

$$J = \frac{1}{2\rho c} \sum_{i=1}^{N} \left| p_t^i \right|^2 \Delta S_i \tag{7}$$

being J the total radiated acoustic power, ρ and c the density and sound velocity of wave in air; p_i the sound pressure values measured at some prescribed measurements points and ΔS_i the surfaces relative to each measurement point. Pressure values are not directly measured, but computed from the signals deriving from the reference sensors positioned on the glazed panel (through the use of filters). Thus, the structural-acoustic coupling is inherent in the definition of the cost function. It was demonstrated by (Fuller et al.,1997) and (Nelson & Elliott, 1992) that substituting the opportune expression of radiated sound pressure, given

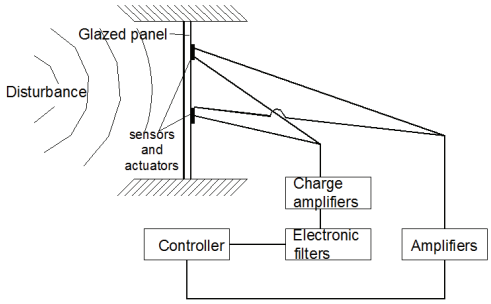

Fig. 5. Scheme of an ASAC system for glazed panels integrated in buildings

by the superposition of the two contributions of both the disturbance and the control actuators, the cost function is scalar. It can be converted into a quadratic expression of complex control voltages, and it was demonstrated that this function has a unique minimum. The general form of the equation to be minimized becomes:

$$J = \underline{h}^T \underline{q} + \underline{c}^T \underline{v}_i \tag{8}$$

where q is the vector of complex input disturbances, h is the vector of transfer functions associated with these disturbances; c is the control transfer function vector and v is the unknown vector. In this way a vector of voltages v_i is computed, minimizing the total radiated field.

Once the transfer functions between the reference signal deriving from reference sensors and the acoustic radiated noise is known for a given system, the control plant will automatically execute all these steps, minimizing the radiated noise even if glazed panels are subject to time-dependent input disturbances, giving back an automated glazed facade, that actively changes its properties according to the disturbance. Before implementing this control system, it is necessary to calculate the control transfer functions, which requires as a preliminary stage, the choice of the opportune kind of secondary sources, carried out in the next section.

However, the analytical model can be implemented only following a series of simplifications, which appear difficult to apply in terms of the actual situations that one can come across in the building field:

- simple support boundary constraints, whereas in fact, constraint situations are more complex and more similar to a semi- fixed or yielding joint;
- applications of only point forces, without the association of mass as occurs in the real case when control is effected through the use of actuators contrasted by stiffening structures.

Given the above considerations, it has been established that the numeric model based on the theory of Kirchhoff-Love, will be substituted by a model built using finite element software programs (ANSYS™, LMS VIRTUAL LAB™), which allows overcoming the simplifications tied to the analytic model.

4.3 Piezoelectric actuators

Two main types of actuators, suitable for glazed facades, are presently marketed (Fig. 6):

- Piezoelectric (PZT) patch actuators providing bending actions to excite structures;
- PZT stack actuators providing point forces to excite structures.

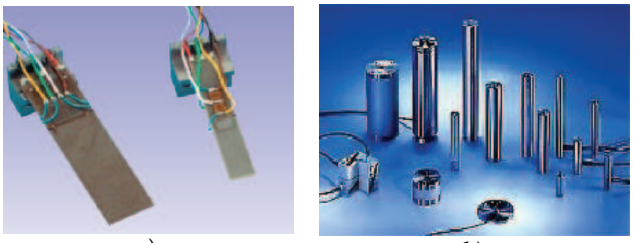

a) b)

Fig. 6. PZT patch (a) and stack actuators for glazed facades (b).

The first type is usually bonded to a surface while the second needs a stiffening structure to fix it and make it transfer forces to a surface for controlling purposes. These actuators are available in a wide range of sizes (from few centimetres to various decimetres) and are capable of generating high forces (with reduced displacements) inside a wide range of frequencies (Dimitriadis, Fuller, Rogers, 1991). Even if they were shown to work properly for many applications, however they have not been tested in applications on glazed facades, and most of the experiments were carried out in the automotive and aeronautic fields of research. As far as concerns the choice of actuators, the first rectangular shaped patch may interfere with visibility (Fig. 7-a); the stack one instead is very small but needs a stiffener in order to work properly (Fig. 7-b).

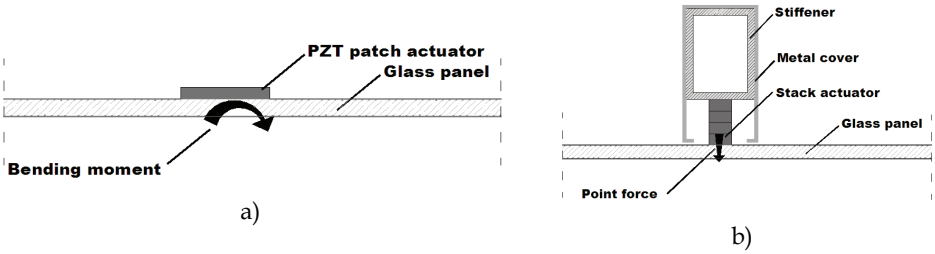

a) b)

Fig. 7. PZT patches (a) and PZT stack actuators (b), as applied on a glass panel.

In the asymmetric disposal of Fig. 7-a, the PZT patch excites the 2D structure with pure bending, that can be simulated with the numerical model developed in (Dimitriadis, Fuller, Rogers, 1991). It is assumed that the strain slope is continuous through the thickness of the glass plate and of the PZT patch, but different along the directions parallel to the plate sides, which in turn are assumed parallel to the coordinate axes (the strain slopes are billed C_x and C_y). The mathematical relation between strain and z-coordinate is:

$$\varepsilon_x = C_x \cdot z \text{ and } \varepsilon_y = C_y \cdot z \tag{9}$$

being the origin of the z-axis in the middle of the plate thickness and ε the strain. The unconstrained strain of the actuator (ε_{pe}) along plate axes is dependent to the voltage applied (V), the actuator thickness (h_a) and the PZT strain constant along x or y directions ($d_x = d_y$):

$$\varepsilon_{pe} = \frac{d_x V}{h_a} \tag{10}$$

Considering that the plate is subject to pure bending, no longitudinal waves will be excited, and by applying the moment equilibrium condition about the centre of the plate along x and y directions as in (Fuller, Elliott, Nelson, 1997), assuming that the plate thickness is $2h_b$, the plate elastic modulus is E_p, the actuator elastic modulus is E_{pe}, and ν_p and ν_{pe} are the Poisson coefficients of the plate and actuators respectively; also assuming that moments induced in the x and y directions (billed with m_x and m_y) are present only under the PZT patch, and assuming that it is located between the points of coordinates (x_1,y_1) and (x_2,y_2), in (Dimitriadis, Fuller, Rogers, 1991) it is shown that:

$$m_x = m_y = C\varepsilon_{pe}\left[H(x-x_1)-H(x-x_2)\right]\left[H(y-y_1)-H(y-y_2)\right] \tag{11}$$

being $H(x)$ the Heaviside function and $C=EIK_f$, where I is the moment of inertia of the plate; then the equation of motion for plates subject to flexural waves can be written:

$$EI\left(\frac{\partial^4 w}{\partial x^4}+\frac{\partial^4 w}{\partial y^4}\right)+\rho h\frac{\partial^2 w}{\partial t^2} = -p(x,y) \tag{12}$$

where p is an external uniform pressure applied on the plate. Eq. (11), if written with the actuator induced moment, becomes:

$$\frac{\partial^2\left[M_x(x)-m_x(x)\right]}{\partial x^2}+\frac{\partial^2\left[M_y(y)-m_y(y)\right]}{\partial y^2}-\omega^2\rho S w = 0 \tag{13}$$

where M is the internal plate moment and m is the actuator induced bending moment; ρ and S are density and surface of the plate; w is the displacement and ω is the wave phase change. Assuming that the actuator is perfectly bonded on the glass plate and substituting (11) inside (13), the solution of (12) can be calculated by using the modal expansion of (3), which gives back:

$$W_{mn} = \frac{4C_0\varepsilon_{pe}}{\rho h mn\,\pi^2\left(\omega_{mn}^2-\omega^2\right)}\left(k_m^2+k_n^2\right)p_1 p_2 \tag{14}$$

where: $p_1 = cos(kmx_1) - cos(kmx_2)$, $p_2 = cos(kny_1) - cos(kny_2)$.

Equation (14) can be written in terms of (3) and (5), defining the variable:

$$P_{mn} = \frac{4C_0\varepsilon_{pe}}{mn\,\pi^2}\left(k_m^2 + k_n^2\right)p_1 p_2 \tag{15}$$

Thus, given the properties of the PZT patches under use and the ones of the plate, (14) together with (5) and (3) gives back the transversal displacement function on the 2D plate caused by PZT patch actuators with respect to *x* and *y* coordinates. In the case shown in Fig. 7-b, the stack actuator has the task of providing a punctual force, instead of a bending moment. Following a procedure similar to the one explained above, it is possible to calculate a numerical model that describes the vibration field in terms of (3) and (5) exploiting the following relation:

$$P_{mn} = \frac{4F_a}{ab}\sin k_m x_f \sin k_n y_f \tag{16}$$

where *a* and *b* are the side lengths of the plate; x_f and y_f are the coordinate of the point where the force F_a is applied, that is the action provided by the stack actuator, which is dependent to the reaction system stiffness. Assuming d_z the strain constant of the actuator along the z-direction, its unconstrained displacement will be computed by:

$$w_a = \frac{d_z V}{L_a} \tag{17}$$

where L_a is its height. In fact the real displacement of the stack is lower than (16) because the reaction system has finite stiffness *K*, and the force effectively exerted by the stack along the z-direction is:

$$F_a = \frac{d_z V K}{1 + \frac{K}{K_a}} \tag{18}$$

being *ka* the actuator stiffness. As in the previous case, the transverse vibration displacement of a 2D plate can be calculated by (14) with (5) and (3).

In the following numerical simulations, performed according to the model described above, the disturbance is assumed to be a wave with frequency near the frequency of the mode of vibration (2,2) of a typical building façade's panel, whose effect is compared with the one given by the use of the two aforementioned kinds of actuators. The glazed panel is supposed to be simply supported along the edges. The two configurations of Fig. 7 are studied analytically. The properties of the glazed plate used for these simulations are listed in Tab. 1, while for PZT patches in Tab. 2. For the simply supported plates of Tab. 1, natural frequencies of vibration are given by (6), whose results are listed in Tab. 3 for the smallest modes; so the frequency of the disturbance was chosen equal to 78 Hz. In the first case of Fig. 7-a, the behaviour of the panel of Tab. 1 is simulated when equipped with two dispositions of PZT patches:

- 8 patches equally distributed 0.05 *m* far from the panel edges;
- 26 patches equally distributed 0.05 *m* far from the panel edges.

Each rectangular shaped patch measures (0.05 x 0.04) *m*. Fig. 8 shows the distribution of the maximum amplitude vibration field along the middle axis of the plate, computed along the y=l/2. One of the diagrams is referred to the effect due to the disturbance wave at frequency v = 78 Hz and intensity 100 dB. For a voltage of 150 V (that is the highest limit for low-voltage actuators) PZT patches can generate vibration fields far lower than the one generated by the disturbance.

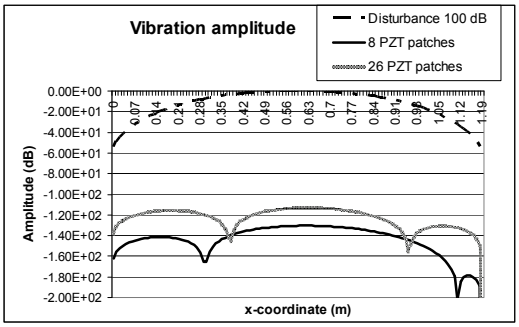

Fig. 8. Amplitude displacement along the y=l/2 axis due to the positioning of PZT patches actuators, normalized with respect to the maximum disturbance value.

In the second case vibration amplitudes are computed for the stack configuration shown in Fig. 7-b. In Fig. 9 such vibration amplitudes are drawn with dependence to the voltage provided to stack actuators. It is assumed that the panel is equipped with 3 actuators (0.02 *m* long with $7.8 \cdot 10^{-5}$ m^2 cross sectional area) per each side, equally spaced and at a 0.03 *m* distance from the two edges; the stiffness of the reaction system is assumed equal to 200 *N/μm*. Fig. 9 shows that, regardless of the small rigidity of the reaction system, the stack actuators can produce a vibration amplitude comparable with the one due to the disturbance with only a voltage of 100 V.

Symbol	QUANTITY	Units of measurement	Value
E_p	Modulus of elasticity	Pa	$6..9 \cdot 10^{10}$
ν_p	Poisson coefficient	-	0.23
ρ_p	density	Kg/m^3	2457
h_p	thickness	m	0.006
l_p	Side length	m	1.2

Tab. 1. Glazed plate's properties.

Symbol	QUANTITY	Units of measurem.	Value
E_{pe}	Modulus of elasticity	Pa	$6.3 \cdot 10^{10}$
ν_{pe}	Poisson coefficient		0.3
ρ_{pe}	density	Kg/m^3	7650
h_{pe}	thickness	m	0.0002
d_{31}	Expansion constant	m/V	-0.000000000166

Tab. 2. PZT patch's properties.

Mode	FREQUENCY (HZ)	Mode	Frequency (Hz)
(1,1)	20.6	(2,2)	82.4
(1,2)	51.5	(2,3)	133.8
(1,3)	102.9	(3,3)	185.2

Tab. 3. Natural frequencies of vibration.

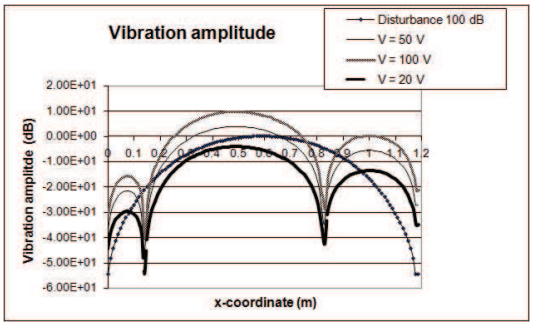

Fig. 9. Amplitude displacement along the y=l/2 axis due to the positioning of stack stiffened actuators, normalized with respect to the maximum disturbance value.

Therefore, given the high controllability provided by stack actuators, they have been considered suitable for controlling glazed facades and they have been object of the experimental campaign and technologic development carried out in this research.

5. The case study: An Active Structural Acoustic control for a window pane

5.1 The components of ASAC System for glazed facades

In paragraph 4.2 the two basic arrangements for an ASAC system configuration have been introduced, that are feed-forward and feed-back types. As already discussed, the first one requires the knowledge of the primary disturbance, which implies the use of a reference microphone. This solution seems to be unpractical for the suggested application, requiring the installation of a microphone on the exterior of the window, unfeasible for functional and aesthetical issues. Hence, the feedback arrangement is preferred by the authors and detailed in the following pages.

The components of a feedback ASAC system for glazed facades are (Fig. 10):

- sensors for detecting vibration (e.g. strain gauges);
- electronic filters for analyzing signals from sensors in order to check the vibration field induced by disturbance;
- an electronic controller for manipulating signals from the sensors and compute the most efficient control configuration at the actuators level;
- charge amplifiers for driving secondary actuators on glazed panels according to the outputs sent by the controller;
- actuators for controlling the vibration field of glazed panels.

As seen in paragraph 4.3 two different kinds of actuators are available, patch and stack actuators. For building applications, feasibility and aesthetical considerations suggest that stack actuators are preferred, as their smaller size interferes less with visibility and transparency and allow them to be easily mounted and dismantled from glass surface.

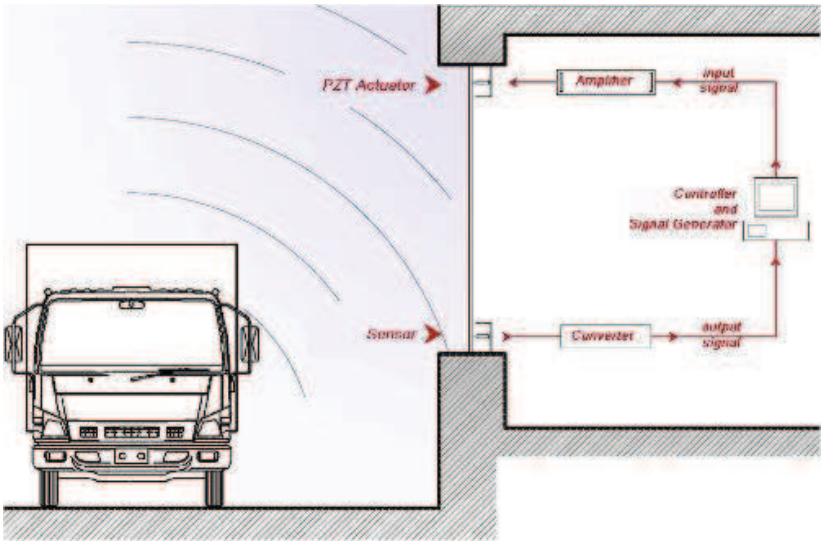

Fig. 10. Layout of the ASAC control system for glazed facades

5.2 The functioning of ASAC System for glazed facades

Signal coming from the sensors is elaborated by charge amplifiers, that convert voltage signals into physical variables like displacements, velocity and accelerations, and by electronic filters, that separate the total vibration field into one due to the primary disturbance from the other connected with the action of secondary sources. The electronic controller, starting from the error signal, estimates the radiated field in some positions of the receiving room and then computes the opportune voltage to be supplied to the actuators in order to reduce the panel's acoustic efficiency. Signal amplifiers provide for necessary electric power.

The optimization of the actuator's actions, in order to minimize the number and the size of the employed sensors and actuators, is derived from opportune algorithms implemented in the controller, like the one presented in (Clark & Fuller, 1992), based on the quadratic linear optimum control theory (see paragraph 4.2). It consists of two parts, the first dedicated to the determination of actuator size and location and the second to sensors. In both parts, the core algorithm computes the voltage to be supplied to the actuators in order to reduce glass vibrations, while the rest of the procedure defines the best actuators' configuration, upon determination of constraints relative to plate's geometry and design choices.

5.3 The technological solution developed as test-case

Stack actuators, as compared to laminated actuators, need a stiffener in order to work properly, hence a technological solution to realize this stiffener has to be designed. The presence of the stiffener, according to its position on the glass surface, may also determine interference problems with the aesthetical appearance of the glass panel which cannot be disregarded. First of all, in order to minimize the radiation efficiency of the vibrating glass surface, the correct positioning of stack actuators has to be studied. Two are the possible ways:

- by decreasing the vibration amplitude of flexural waves (Fig. 11-a);
- By changing the original vibration in order to obtain a vibration field where only even modes dominate (Fig. 11-b).

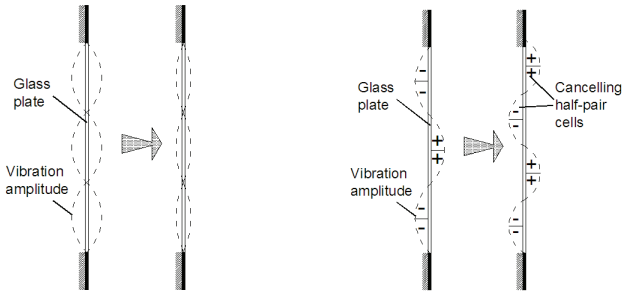

a) b)

Fig. 11. Reduction of the overall acoustic radiation efficiency

In the first case actuators should act in order to reduce vibration amplitudes, while in the second one they should generate a vibration field with less radiation efficiency. To each of the alternatives listed corresponds a different positioning of actuators: in the first case they have to be installed in the points where maximum vibration amplitudes are monitored, while, in the second one, they have to be moved along the border lines, with less interference in glass panel's appearance. Starting from these considerations, in Fig. 12 three possible technological solutions are depicted (Naticchia and Carbonari, 2007):

a. stack actuators positioned close to the central axis, usually characterized by maximum amplitude vibrations, and stiffened by a metal profile (approach 1);
b. stack actuators installed along one border of the panel and stiffened by an angular profile (approach 2);
c. stack actuators placed close to the borders and stiffened with point reaction systems (approach 3).

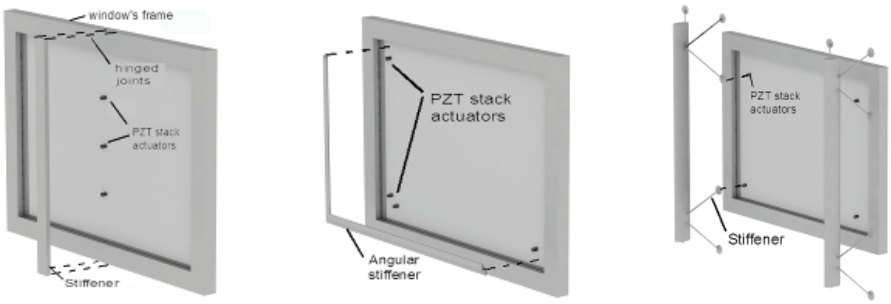

a) b) c)

Fig. 12. Technologic solutions suggested for the installation of actuators.

Further proposals for technological solutions have been advanced, where the actuator is contrasted by a point reaction system directly attached to the glass panel's surface. For this purpose, the use of two different kinds of metallic profiles have been hypothesized: in Fig. 13-a a circular-shaped profile contrasting a stack actuator is depicted in a 3-D view and a

cross-section view, while Fig. 13-b represents a similar solution realized with a z-shaped profile. Both hypotheses seem to be advantageous from an aesthetical point of view, showing little interference with visibility through the glass, and should be studied relative to profile characteristics and to the stress induced in correspondence of the connection point between the same profile and the glass panel.

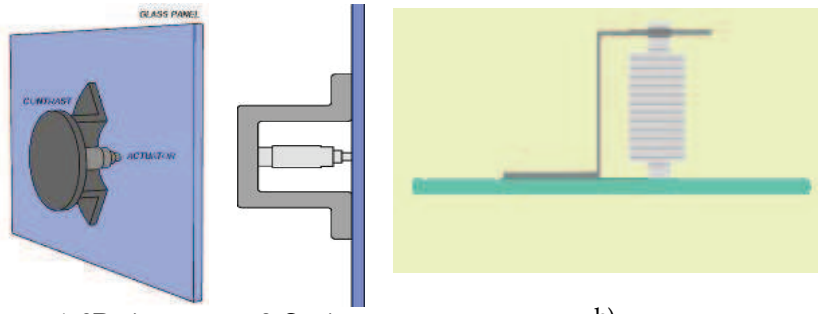

a-1: 3D view a-2: Section b)

Fig. 13. Further hypotheses of point reaction systems: circular-shaped profile (a-1;a-2); Z-shaped profile (b).

For the acoustic simulations carried out and discussed in this chapter, in order to evaluate the effectiveness of the purposed technology over the limits imposed by the choice of one solution with respect to another, an experimental solution has been developed, employing a stack actuator, stiffened by a mass, realized with a cylinder of metallic material overlapped and connected to the free extreme of the actuator, as will be detailed in paragraph 6.2.

6. Experimental analysis

In the following paragraphs, the results of experimental and numerical analyses carried out to evaluate acoustic improvements deriving from the application of the suggested active control technology will be presented (Carbonari and Spadoni, 2007). For this purpose, a finite element model and an experimental prototype were built: in both models the stiffener has been simulated with a 0.177 *Kg* weighted mass contrasting the free extreme of the actuator (Fig. 15-e and 15-f).

6.1 The building of the experimental prototype

Experimental simulations were performed on a prototype, realized by assembling a (1.00x1.40) *m* sized glazed pane with an aluminium profile frame. The main problem regarding the realization of the prototype was the simulation of a simply supporting boundary constraint: it was pursued with the interposition of two cylindrical Teflon bars between the glass panel and the two window frame profiles, as can be seen in Fig. 14-a. Every screw fixing the glass panel in the window frame was subjected to the same torque (through the use of a dynamometric spanner) equal to 0.1 *N·m*, in order to guarantee uniform contact between the glass and the Teflon bars. The whole system, as shown in Figure 14-b, was placed over dumping supports in correspondence of each panel edge, to avoid the influence of external actions on the glass's vibrations, establishing the simplest boundary conditions. A seventy-seven point grid was defined on the panel, in order to identify measurement marks.